

# Selective Production of Reactive and Nonreactive Oxygen Atoms on Pd(001) by Rotationally Aligned Oxygen Molecules\*\*

Luca Vattuone,\* Andrea Gerbi, David Cappelletti, Fernando Pirani, Roberto Gunnella, Letizia Savio, and Mario Rocca

The improvement of product yields is one of the most important goals for surface science, which is a discipline that aims at a thorough understanding of heterogeneous catalysis and the future design of knowledge-based catalysts.<sup>[1]</sup> Simple reactions, such as dissociative O<sub>2</sub> adsorption<sup>[2]</sup> and CO oxidation,<sup>[3]</sup> feature among the most frequently studied processes because of their paradigmatic role and apparent simplicity. The elementary steps of simple chemical reactions<sup>[1–4]</sup> can be studied by performing state-resolved experiments with supersonic molecular beams (SMBs). As recently demonstrated, this technique also allows the exploration of the influence of the rotational alignment of the reactants<sup>[5–6]</sup> by performing an accurate velocity selection of the molecules that are seeded in lighter inert carriers.<sup>[7]</sup>

We previously applied this method, the so-called collisional alignment, to investigate the sticking probability *S* in gas–surface interactions, and found large stereodynamical effects in the presence of preadsorbed molecules, but no effects for molecules that interacted with bare surfaces. Herein we show that, even if the value of *S* is the same, the different rotational alignments of incoming O<sub>2</sub> in the gas phase governs the dissociation process on Pd(001) and is responsible for the generation of oxygen atoms that are

characterized by totally different reactivity towards CO oxidation. CO is connected to a different site above and/or below the surface, which is reached by the O atoms that result from dissociation, as shown by photoelectron diffraction (PD). This phenomenon occurs even at low coverage, thus contradicting state-of-the-art DFT predictions, which show that only on-surface sites should be populated.<sup>[8]</sup> Collisional alignment can thus be envisaged as a tool to tune chemical reactivity in surface chemistry by selectively populating subsurface sites without saturating the on-surface sites and thus opening up new and possibly promising reaction paths.<sup>[9]</sup>

According to previous results, O<sub>2</sub> chemisorbs dissociatively on Pd(001) in the low-coverage limit, the resulting adatoms are situated in fourfold hollow sites and form a disordered layer or a p(2×2) structure, depending on the coverage.<sup>[10]</sup> CO adsorbs randomly at bridge sites, except close to 0.5 monolayers (ML) when a c(2×4) overlayer forms (1 ML = 1.33 × 10<sup>15</sup> Pd atoms cm<sup>−2</sup>).<sup>[11]</sup> CO oxidation has been widely investigated;<sup>[12–13]</sup> the reaction is thermally activated and occurs by a Langmuir–Hinshelwood mechanism and tends to be incomplete,<sup>[14,15]</sup> since some O<sub>2</sub> and some CO desorption are observed up to initial coverages of 0.25 ML for both reactants.<sup>[14]</sup>

We performed state-resolved experiments<sup>[16]</sup> by exploiting rotationally polarized SMBs: the forward collisions in the supersonic expansion of a seeded mixture (4% O<sub>2</sub>, 96% He in the present experiments) generate very low rotational temperatures, which correspond to the population of low rotational **K** states (mainly *K* = 1), and molecular beam polarization, that is, the selective population of the *m* helicity states.<sup>[17]</sup> The **K** polarization is related to the alignment of the molecular axis with respect to the beam direction and its degree depends strongly on the final speed reached by the molecules<sup>[7]</sup> after the supersonic expansion. The selection of a specific portion of the SMB velocity distribution thus allows a definite degree of alignment of the oxygen molecules to be singled out.<sup>[7,18,19]</sup> A two-disk velocity selector was used in order to maximize the throughput and thus enable retarded reflector measurements.<sup>[16]</sup> The fast tail (FT) of the SMB velocity distribution consists mostly of molecules in the helicity state *m* = 0, while the rotational axes of the molecules that form the slow tail (ST) are distributed isotropically (similar population of *m* = 0 and *m* = ±1 components, *K* = 1 is the most populated level). Since the beam impinges along the surface normal, the *m* = 0 and *m* = ±1 states correspond to molecules that rotate as cartwheels (CWs) or as helicopters (HEs), respectively, with respect to the surface plane.<sup>[20]</sup> This result implies that the ST consists mainly of HEs.

[\*] Dr. L. Vattuone, Dr. A. Gerbi  
Dipartimento di Fisica dell'Università di Genova and CNISM  
Via Dodecaneso 33, 16146 Genova (Italy)  
Fax: (+39) 010-314-218  
E-mail: vattuone@fisica.unige.it  
Homepage: <http://www.fisica.unige.it/~vattuone/>  
Prof. D. Cappelletti  
CNISM Unità di Perugia and Dipartimento di Ingegneria Civile ed Ambientale Università di Perugia  
Via G. Duranti, 93, 06125 Perugia (Italy)  
Prof. F. Pirani  
CNISM Unità di Perugia and  
Dipartimento di Chimica Università di Perugia  
Via Elce di Sotto 8, 06123 Perugia (Italy)  
Prof. R. Gunnella  
CNISM, Dipartimento di Fisica, Università di Camerino  
Via Madonna delle Carceri, 62032 Camerino (Italy)  
Dr. L. Savio, Prof. M. Rocca  
Dipartimento di Fisica dell'Università di Genova and IMEM-CNR  
Via Dodecaneso 33, 16146 Genova (Italy)

[\*\*] We thank K. Reuter and S. de Gironcoli for scientific discussions on DFT and technical assistance from the SuperESCA staff. We also thank G. Ertl, G. J. Kroes, and D. A. King for critical reading of the manuscript. Financial support by Compagnia S. Paolo is acknowledged.

Supporting information for this article is available on the WWW under <http://dx.doi.org/10.1002/anie.200900870>.

The CO<sub>2</sub> yield and O<sub>2</sub> sticking probability versus time for O<sub>2</sub> exposures on CO pre-covered Pd(001) at two different surface temperatures  $T_s$  are shown in Figures 1a and b,

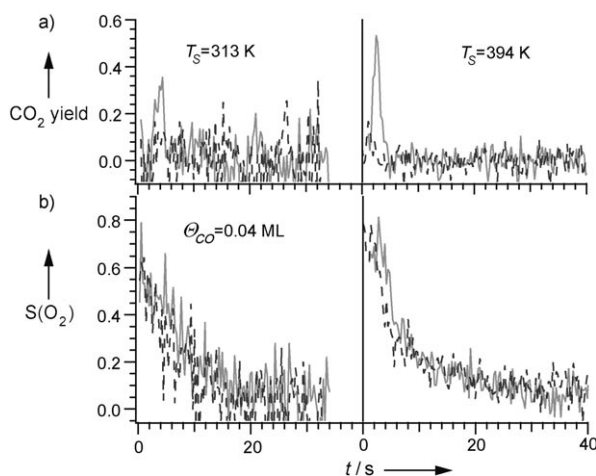


**Figure 1.** a) CO<sub>2</sub> yield and b) O<sub>2</sub> sticking probability as a function of time for O<sub>2</sub> molecules from the ST (—) and FT (---) on Pd(001) pre-covered with 0.04 ML of CO at 313 K (left) and 394 K (right). The traces for the CO<sub>2</sub> yield are corrected for the different ionization factor of O<sub>2</sub> and CO<sub>2</sub>, so that the intensities can be directly compared.  $S(O_2)$  is isotropic with respect to the investigated beam tail while CO<sub>2</sub> production is not. The zeros for  $S(O_2)$  and the CO<sub>2</sub> yield are determined by the level at which the QMS signal is no longer distinguishable from the level before dosing. Negative values are due to noise fluctuations.

respectively. The pre-coverage was set at  $\Theta_{CO} = 0.04\text{ ML}$ , so that most of the O<sub>2</sub> molecules interacted with the bare surface<sup>[21]</sup> and the sticking probability was large.<sup>[6]</sup> If  $T_s$  is high enough for CO to be mobile and for the reaction barrier to be overcome, the O adatoms react and give rise to CO<sub>2</sub> desorption. It is clear from Figure 1 that the CO<sub>2</sub> desorption yield is larger for molecules in the ST than for those in the FT. The integrated CO<sub>2</sub> production is given in Table 1. At  $T_s =$

**Table 1:** Total amount of desorbing CO<sub>2</sub>.<sup>[a]</sup>

	Total CO <sub>2</sub> yield (ML) $T_s = 313\text{ K}$	Total CO <sub>2</sub> yield (ML) $T_s = 394\text{ K}$
ST	(0.020 ± 0.006)	(0.018 ± 0.002)
FT	(0.005 ± 0.006)	(0.004 ± 0.002)

[a] The errors correspond to a 99% confidence level. Any possible systematic error in the absolute value of the flux affects all the values by the same factor. The total O<sub>2</sub> uptake at the end of the reaction (after 5 s at  $T_s = 394\text{ K}$ ) corresponds to an oxygen atom uptake of 0.12 ML.

394 K the production corresponds to the removal of about half of the CO ad molecules for the ST, while only one tenth are consumed after the same exposure to the FT. The remaining CO is consumed over a longer timescale. Considering the error bar in the measured CO<sub>2</sub> yield and in the degree of alignment, these numbers are consistent with the fraction of helicopters present in the ST ((58 ± 5) %), and the FT ((33 ± 5) %; see the Supporting Information). It can thus

be concluded that only the HEs generate the reactive oxygen species.

We further noticed that CO<sub>2</sub> production started only after a small but measurable delay, which implied that only O atoms generated for O<sub>2</sub> uptakes larger than approximately 0.02 ML are reactive.<sup>[22]</sup> To investigate this phenomenon further, the surface, which was precovered with CO at 313 K, was exposed to the ST or the FT of the O<sub>2</sub> SMB (see Figure 2);

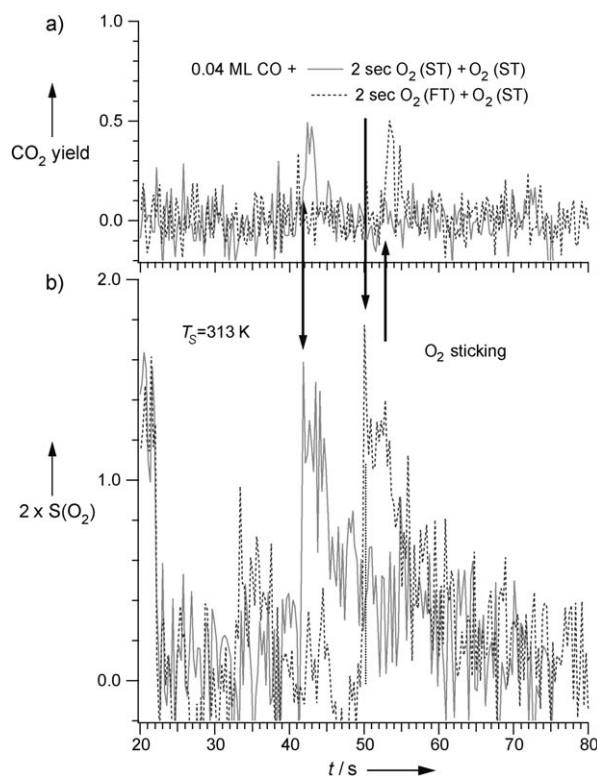


**Figure 2.** a) CO<sub>2</sub> yield and b) oxygen sticking probability ( $2 \times S_{O_2}$ ) as a function of time. A 0.04 ML CO pre-covered surface is initially exposed to O<sub>2</sub> either from the ST (—) or by FT (---) for a time shorter than the ignition time. The exposure is eventually resumed with the ST, after 42 s for the ST pre-treatment and after 50 s for the FT pre-treatment (this difference does not affect the final outcome). CO<sub>2</sub> desorption occurs without delay if the surface was pre-dosed with the ST, while a significant delay, as if no O pre-adsorption had been performed, is observed for the FT.

the dose was interrupted shortly before CO<sub>2</sub> production for the ST starts. After a delay of some tens of seconds, the exposure was resumed, with the ST used in both cases. CO<sub>2</sub> emission was then observed to start immediately if the first pulse was ST, while a measurable delay, as if the sample had not been pre-exposed, was present if the first pulse was FT. The presence of a delay proves that: 1) the states of the oxygen atoms generated in the pre-treatment are different for the ST and the FT; 2) these oxygen atoms are stable for the time of the experiment at  $T_s = 313\text{ K}$ ; and 3) only pre-treatment with the ST is effective for initiating CO oxidation. If, as can be reasonably expected, the delay is due to the saturation of surface defects, it is concluded that the defects cannot be reached by the O atoms generated from the FT.

In order to directly probe the adsorption sites of the different oxygen moieties, we investigated O<sub>2</sub> adsorption on bare Pd(001) by PD at the SuperEsca beamline of the Elettra Synchrotron Light Source in Trieste, which is equipped with a velocity selected SMB. Since the X-ray photoelectron spectroscopy (XPS) energies of the O 1s and Pd 3p<sub>3/2</sub> levels overlap, the photoemission information was retrieved from the O 2s peak. Additional O 2s intensity that arises from adsorbed CO is shifted by 6.5 eV and is therefore clearly discernible. However, CO adsorption from the residual gas was always negligible, as also confirmed by inspection of the C 1s region.

Figure 3 shows the O 2s photoemission spectra recorded at  $T_s = 220$  K (when removal of O by background CO is thermally hindered, even on a timescale of several hours) with

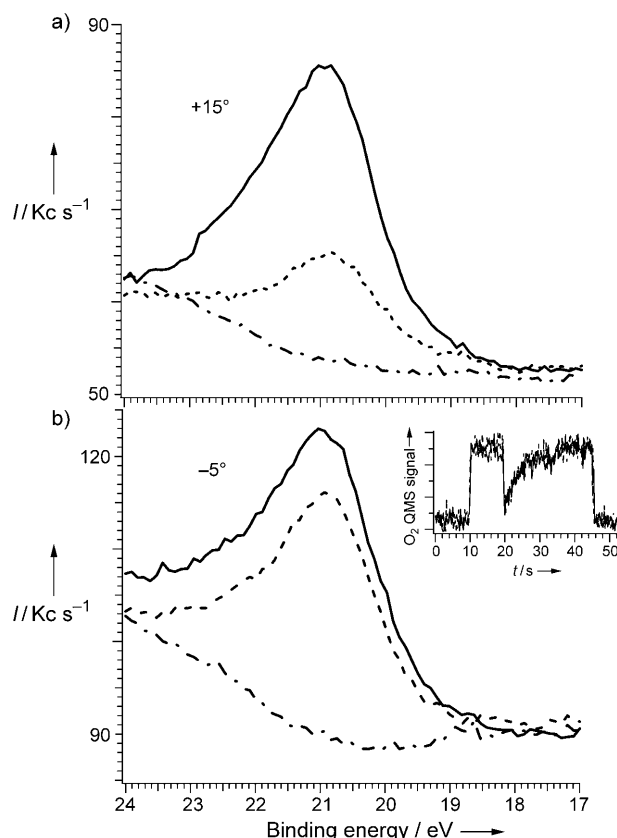


**Figure 3.** Photoemission spectra of the O 2s level recorded on Pd(001) at  $T_s = 220$  K versus binding energy. The curves show the clean surface (---) and after dosing 0.10 ML of O<sub>2</sub> by ST (—) or FT (···). In both cases the estimated atomic O coverage is 0.12 ML. The different count rates at the different angles and the low signal for the FT at +15° should be noted. The inset shows O<sub>2</sub> uptake for the ST and the FT on the bare surface at normal incidence, which proves that the coverage is independent of the rotational alignment.

a photon energy  $h\nu = 150$  eV for two different photoemission polar angles  $\theta$  along the [110] direction. The spectra correspond to the bare surface (---) and to oxygen layers obtained after exposure to 0.10 ML O<sub>2</sub> at normal incidence with ST (—) and FT (···), respectively. The estimated atomic O coverage is 0.12 ML. The inset in Figure 3 shows

that, within experimental error, the O<sub>2</sub> uptakes are identical for the two tails. In spite of this, it is apparent that the photoemission intensities are different, thus confirming that most of the O atoms that originated from the ST and FT occupy different sites.

Figure 4 shows the contribution of HEs and CWs as a function of  $\theta$  (dashed curves) deconvoluted from the measured intensity for the ST and FT at 0.12 ML coverage

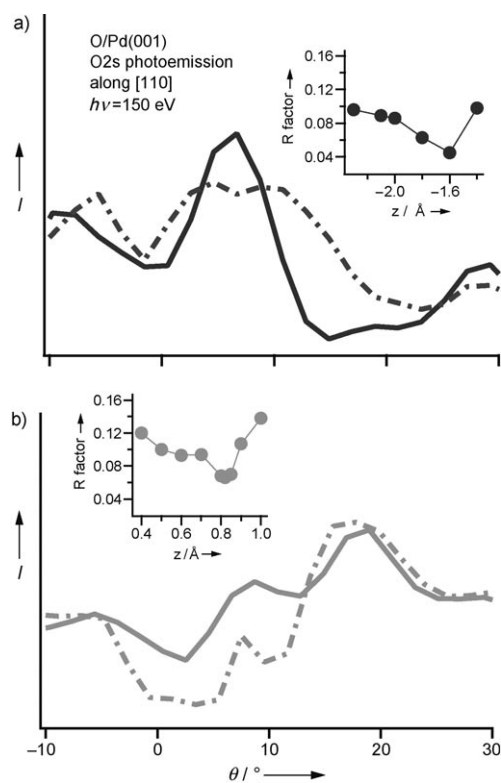


**Figure 4.** Deconvoluted experimental PD intensities of the O 2s level versus electron emission angle (with respect to the surface normal) for a) CW (---) compared with the theoretical fit of the octahedral model (—) and b) HE (---) compared with the theoretical fit of the fourfold hollow model (—). The photon energy is 150 eV and the detection direction is along the [110] azimuth. Further photoemission data recorded versus photon energy are presented in the Supporting Information. The insets show the R factors versus adsorption height.

according to the rotational polarization (see the Supporting Information). By comparison with multiple scattering calculations (continuous lines)<sup>[23]</sup> of the angular anisotropy, we found that the best agreement for HEs is with oxygen in the fourfold hollow site (O<sub>four</sub>), which is  $(0.82 \pm 0.02)$  Å above the Pd surface plane. The location of this site is consistent with previous experimental and theoretical studies.<sup>[8,24]</sup> For CWs, however, the only compatible site is the octahedral interstitial (O<sub>octa</sub>) with the O atoms sitting  $(1.60 \pm 0.10)$  Å below the surface plane and inducing a deformation of the surface atomic geometry, to attain a Pd–O distance of about  $(2.0 \pm 0.10)$  Å. The errors are related to the clear-cut minima in the R factors (see insets in Figure 4) which, in turn, are due to the high sensitivity to the atomic geometry for the scattering of the photoelectrons in the present conditions.

The reactivity of HE-generated oxygen (or passivity of CW-generated oxygen) towards CO descends naturally from the location above (or below) the surface of such atoms. A subsurface location of most of the CW-generated O atoms may appear surprising and is indeed not supported by DFT calculations.<sup>[8]</sup> We note nevertheless that the occupation of hollow and octahedral sites is similar to that observed for O–Pd(111),<sup>[25]</sup> for which both the face-centered cubic (fcc) hollow sites (predicted by DFT calculations) and the octahedral sites (produced by filling a subsurface defect) were reported. The occurrence of nonequilibrium conditions, which may elude a static DFT investigation, must be taken into consideration, thus a proper dynamical approach is called for. This site occupation may arise because of the release of energy (several eV) in the chemisorption process, which results in the generated O atoms. Their velocity is mainly parallel to the surface for HEs and at an angle to the surface for CWs, which causes implantation into the surface in the latter case. Finally, the molecules have a translational energy of 0.4 eV and, because of the absence of an activation barrier for adsorption, part of the energy can be employed to overcome the barrier between on-surface and subsurface sites. In agreement with this picture, we observe no stereosensitivity in the reactivity when dosing with O<sub>2</sub> at  $T_s = 730$  K. We mention finally that subsurface-site occupation at low coverage for O/Pd(001) was suggested previously<sup>[26]</sup> to account for the temperature dependence of the oxygen Auger signal. In conclusion, we have demonstrated that the rotational alignment of the incoming O<sub>2</sub> molecules for O<sub>2</sub>–CO/Pd(001) with respect to the surface unexpectedly controls the occupation of different surface sites by atomic oxygen, these sites being characterized by a remarkably different chemical reactivity.

Received: February 13, 2009

Revised: April 28, 2009

Published online: May 28, 2009

**Keywords:** chemisorption · heterogeneous catalysis · palladium · stereodynamics · supersonic molecular beams

- [1] G. Ertl, *Adv. Catal.* **2000**, *45*, 1–69.
- [2] T. Zambelli, J. V. Barth, J. Winterlin, G. Ertl, *Nature* **1997**, *390*, 495–497.
- [3] P. D. Szuromi, *Science* **2007**, *317*, 297.
- [4] M. Bonn, S. Funk, C. Hess, D. N. Denzler, C. Stampfl, M. Scheffler, M. Wolf, G. Ertl, *Science* **1999**, *285*, 1042–1045.
- [5] L. Vattuone, A. Gerbi, M. Rocca, U. Valbusa, F. Pirani, F. Vecchiocattivi, D. Cappelletti, *Angew. Chem.* **2004**, *116*, 5312–5315; *Angew. Chem. Int. Ed.* **2004**, *43*, 5200–5204.
- [6] A. Gerbi, L. Savio, L. Vattuone, F. Pirani, D. Cappelletti, M. Rocca, *Angew. Chem.* **2006**, *118*, 6807–6810; *Angew. Chem. Int. Ed.* **2006**, *45*, 6655–6658.
- [7] V. Aquilanti, D. Ascenzi, D. Cappelletti, F. Pirani, *Nature* **1994**, *371*, 399–402.
- [8] E. Lundgren, J. Gustafson, A. Mikkelsen, J. N. Andersen, A. Stierle, H. Dosch, M. Todorova, J. Rogal, K. Reuter, M. Scheffler, *Phys. Rev. Lett.* **2004**, *92*, 046101; J. Belilev, K. Reuter, unpublished results: this more recent DFT investigation also shows the subsurface location of oxygen to be unstable.
- [9] A. D. Johnson, S. P. Daley, A. L. Utz, S. T. Ceyer, *Science* **1992**, *257*, 223–225.
- [10] K. H. Rieder, W. A. Stocker, *Surf. Sci.* **1985**, *150*, L66–L70.
- [11] J. C. Tracy, W. Palmberg, *J. Chem. Phys.* **1969**, *51*, 4852–4862.
- [12] See for example, G. Ertl, *Surf. Sci.* **1994**, *299–300*, 742–754.
- [13] C. J. Zhang, P. Hu, *J. Am. Chem. Soc.* **2001**, *123*, 1166–1172.
- [14] E. M. Stuve, R. J. Madix, C. R. Brundle, *Surf. Sci.* **1984**, *146*, 155–176.
- [15] Y. Ohno, T. Matsushima, K. Shobatake, H. Nozoye, *Surf. Sci.* **1992**, *273*, 291–300.
- [16] A. Gerbi, L. Vattuone, M. Rocca, U. Valbusa, F. Pirani, D. Cappelletti, F. Vecchiocattivi, *J. Chem. Phys.* **2005**, *123*, 224709.
- [17] The O<sub>2</sub> molecule belongs to Hund's case (b): the electronic spin **S** (with  $S=1$ ), which is ultimately responsible of molecular paramagnetism, adds to the rotational angular momentum **K** to give three possible values for the total angular momentum **J**. Only odd values are allowed for *K* since O<sub>2</sub> has no nuclear spin. Under the present conditions,<sup>[18]</sup> more than 90 % of the molecules are in the  $K=1$  state. The helicity quantum number *m* is defined as the quantized projection of **K** with respect to the SMB propagation direction.
- [18] V. Aquilanti, D. Ascenzi, D. Cappelletti, S. Franceschini, F. Pirani, *Phys. Rev. Lett.* **1995**, *74*, 2929–2932.
- [19] V. Aquilanti, D. Ascenzi, M. Bartolomei, D. Cappelletti, S. Cavalli, M. D. Vitores, F. Pirani, *Phys. Rev. Lett.* **1999**, *82*, 69–72.
- [20] The definition of cartwheel and helicopter motions implies the assumption of the classical concepts of a continuous angular distribution of the rotational angular momenta. This is meaningless in a strongly quantized system such as the present one, but the CW and HE concepts are still used here because they are intuitive in surface scattering processes.
- [21] At large CO pre-coverage, S<sub>O2</sub> depends on the velocity tail (see also Ref. [6]). This is not yet the case for  $\Theta_{CO} = 0.04$  ML.
- [22] The O pre-coverage needed to start CO<sub>2</sub> release decreases with temperature and is compatible with a higher adsorption energy of O at step sites (resulting in a lower oxidation rate) and with temperature-dependent diffusion of the reactants.
- [23] R. Gunnella, F. Solal, D. Sebilliau, C. R. Natoli, *Comput. Phys. Commun.* **2000**, *132*, 251.
- [24] D. Kolkthoff, D. Jurgens, C. Schwennicke, H. Pfner, *Surf. Sci.* **1996**, *365*, 374–382.
- [25] R. Rose, A. Borg, T. Mitsui, D. F. Ogletree, M. Salmeron, *J. Chem. Phys.* **2001**, *115*, 10927–10934.
- [26] S. L. Chang, P. A. Thiel, *J. Chem. Phys.* **1988**, *88*, 2071.